OPEN ACCESS
CellPress

Cell Reports
Report

Sox2 Cooperates with Lkb1 Loss in a Mouse Model of Squamous Cell Lung Cancer

Anandaroop Mukhopadhyay,[1] Kristofer C. Berrett,[1] Ushma Kc,[1] Phillip M. Clair,[1] Stelian M. Pop,[1] Shamus R. Carr,[2] Benjamin L. Witt,[3] and Trudy G. Oliver[1,*]
[1]Department of Oncological Sciences, University of Utah and Huntsman Cancer Institute, Salt Lake City, UT 84112, USA
[2]Department of Surgery, School of Medicine, University of Utah, Salt Lake City, UT 84112, USA
[3]ARUP Laboratories, Department of Pathology, School of Medicine, University of Utah, Salt Lake City, UT 84112, USA
*Correspondence: trudy.oliver@hci.utah.edu
http://dx.doi.org/10.1016/j.celrep.2014.05.036

SUMMARY

Squamous cell carcinoma (SCC) of the lung is the second most common subtype of lung cancer. With limited treatment options, the 5-year survival rate of SCC is only 15%. Although genomic alterations in SCC have been characterized, identifying the alterations that drive SCC is critical for improving treatment strategies. Mouse models of SCC are currently limited. Using lentiviral delivery of *Sox2* specifically to the mouse lung, we tested the ability of *Sox2* to promote tumorigenesis in multiple tumor suppressor backgrounds. Expression of *Sox2*, frequently amplified in human SCC, specifically cooperates with loss of *Lkb1* to promote squamous lung tumors. Mouse tumors exhibit characteristic histopathology and biomarker expression similar to human SCC. They also mimic human SCCs by activation of therapeutically relevant pathways including STAT and mTOR. This model may be utilized to test the contribution of additional driver alterations in SCC, as well as for preclinical drug discovery.

INTRODUCTION

Lung cancer is a leading cause of cancer-related deaths in the United States and worldwide. Squamous cell carcinoma (SCC) is the second most common type of lung cancer, representing ~30% of cases and over 400,000 deaths worldwide each year (Cancer Genome Atlas Research Network, 2012; Jemal et al., 2011). Currently, the 5-year survival rate for SCC is approximately 15%. One of the major problems contributing to treatment failure is a lack of targeted therapies. Targeted therapies that are effective against adenocarcinoma, the other major subtype of non-small-cell lung cancer (NSCLC), are ineffective or contraindicated for SCC. The current standard of care for SCC involves surgery when operable, or combination chemotherapy, usually a platinum doublet, which has a poor response rate (Oliver et al., 2013). Identification of new therapeutic targets for SCC requires elucidation of the critical genes and pathways driving this disease.

Cancer Genome Atlas Research Network (2012) recently sequenced 178 human SCCs, identifying numerous genetic alterations that may serve as valuable therapeutic targets. However, SCC has one of the highest mutation rates of all tumor types, making it difficult to distinguish "driver" from "passenger" mutations. Some genetic alterations in SCC occur in proteins for which targeted therapies are available, such as fibroblast growth factor receptor (FGFR) and phosphatidyl inositol 3-kinase (PI3K)/AKT. Other potential oncogenic drivers were discovered for which there are currently no available therapies, such as the transcription factors SOX2, P63, and NRF2 (Cancer Genome Atlas Research Network, 2012).

Mouse models of adenocarcinoma and small cell lung cancer (SCLC) have been utilized to understand mechanisms of tumor initiation, progression, and therapeutic response (Kwon and Berns, 2013). Genetic models of SCC have only recently been generated (Ji et al., 2007; Xiao et al., 2013). The combination of $Kras^{G12D}$ expression and *Lkb1* loss in the mouse lung leads to lung tumors of multiple lineages (adenocarcinoma, mixed adenosquamous, squamous, and large cell) (Jackson et al., 2001; Ji et al., 2007). While *KRAS* is commonly mutated in human lung adenocarcinomas (~21%), it is rarely altered in SCC (~6%) (Perez-Moreno et al., 2012). In the mouse lung, $Kras^{G12D}$ expression alone promotes the exclusive development of lung adenocarcinomas (Jackson et al., 2001). *LKB1* (also known as serine/threonine kinase 11; *STK11*), a tumor suppressor implicated in metabolism, cell polarity, and growth control, is lost or mutated in 5%–19% of human SCCs (Ji et al., 2007; Perez-Moreno et al., 2012; Shackelford and Shaw, 2009). This suggests that *Lkb1* loss in the $Kras^{G12D/+}Lkb1^{fl/fl}$ model contributes to the altered spectrum of lung tumor types, including squamous tumors.

Recently, a kinase-dead *IKK*α knockin mouse was reported to develop lung SCCs (Xiao et al., 2013). This discovery followed other mouse models with loss-of-function *IKK*α alleles that developed papillomas and skin SCC (Liu et al., 2012). The kinase-dead *IKK*α knockin mice develop spontaneous SCCs of the lung but also develop tumors in the skin, forestomach, and esophagus, contributing to early mortality (Xiao et al., 2013). When wild-type *IKK*α expression is restored using a skin promoter, mice survive longer and develop lung SCCs but still have defects in the forestomach and esophagus. These phenotypes are consistent with the observation that IKKα is

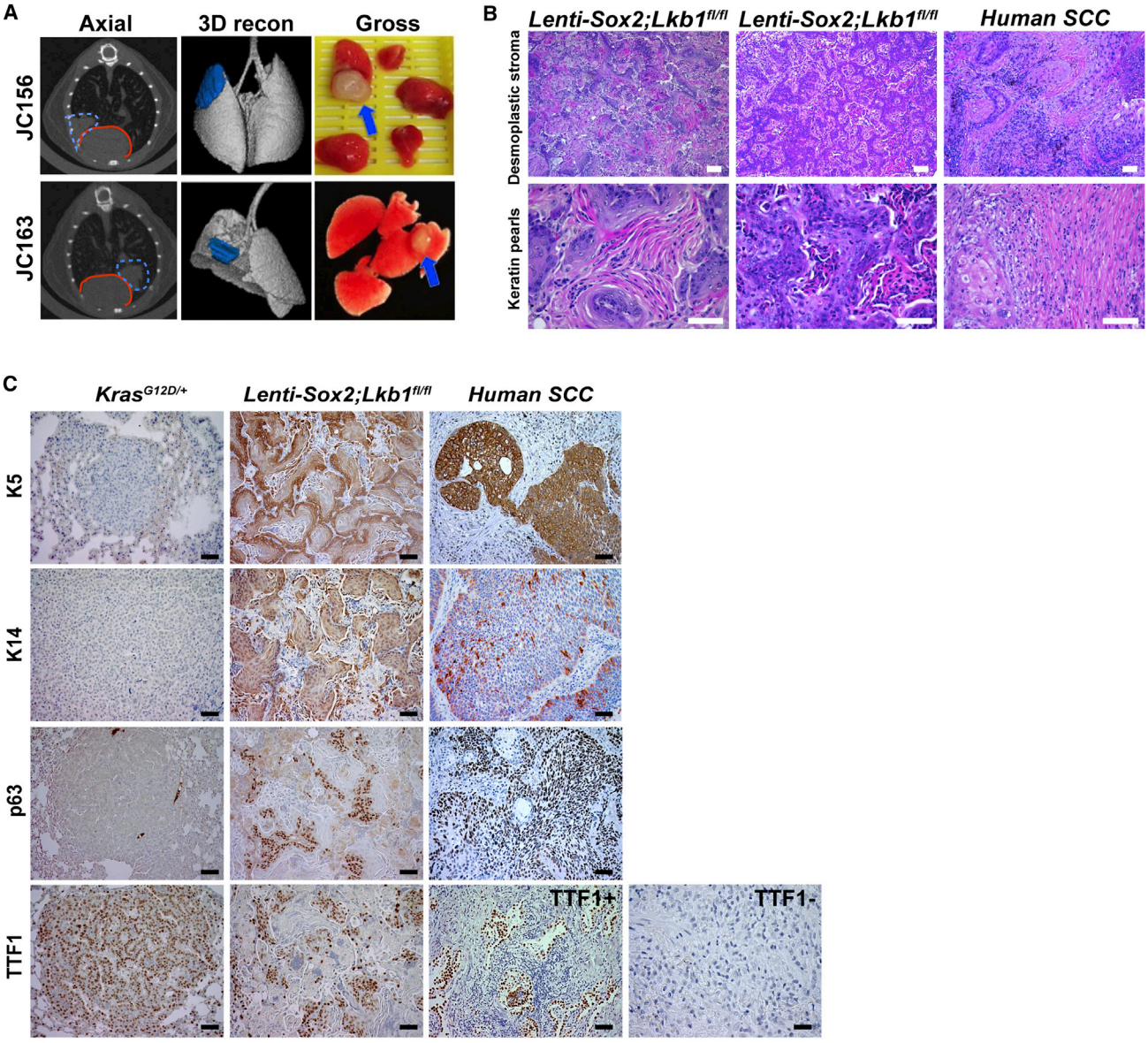

(legend on next page)

downregulated in human skin SCC and in head and neck SCC (Liu et al., 2012), but the role of IKKα in lung SCC is less clear. Copy number losses and genomic mutations in *IKKα* are rare in human lung SCCs, and other mechanisms of altering *IKKα* and its related pathways are not well defined (Cancer Genome Atlas Research Network, 2012). The broad spectrum of lung tumor types in *Kras*$^{G12D/+}$*Lkb1*$^{fl/fl}$ mice and the extrapulmonary phenotypes in the kinase-dead *IKKα* mice make the study of biomarkers, mechanisms of progression, and squamous-specific therapies difficult.

SOX2 is one of the most frequently altered genes in human SCC, amplified in ~21% and overexpressed in 60%–90% of tumors (Bass et al., 2009; Brcic et al., 2012; Cancer Genome Atlas Research Network, 2012; Hussenet et al., 2010). SOX2 is also frequently expressed in early-stage SCC, suggesting that SOX2 expression may be an initiating event in SCC development (Bass et al., 2009; Brcic et al., 2012; Hussenet et al., 2010). Gain-of-function and loss-of-function studies have previously underscored a critical role for Sox2 in lung development, specifically its importance in the proliferation and differentiation of basal and neuroendocrine cells (Gontan et al., 2008; Lu et al., 2010; Que et al., 2009). Consistent with this observation, *SOX2* amplification is common in SCC and SCLC, lung tumors that are thought to originate from basal and neuroendocrine cells, respectively (Bass et al., 2009; Hussenet et al., 2010; Rudin et al., 2012). However, expression of Sox2 alone in the lung promotes hyperplasia and tumors of the adenocarcinoma lineage with aberrant basal cell marker expression (Lu et al., 2010). Although *SOX2* is one of the most frequent genetic alterations associated with human SCC, it has not yet been shown to promote squamous lung tumors in vivo. Here, we sought to identify combinations of gene drivers that promote lung SCC.

RESULTS AND DISCUSSION

Lentiviral Approach to Identify Combinatorial Drivers of Lung SCC

To identify genetic combinations that facilitate *Sox2*-driven SCC, we used a lentiviral approach to combine *Sox2* expression with loss of distinct tumor suppressor genes. Bicistronic lentiviruses expressing *Sox2* and *Cre recombinase* are delivered specifically to the mouse lung using intranasal inhalation, allowing constitutive expression of two genes driven by β-*Actin* and *Pgk* promoters, respectively. Lentiviruses are administered to mice harboring conditional *LoxP*-flanked (“floxed”) tumor suppressor alleles to simultaneously create two genetic “hits”: expression of *Sox2* via the lentivirus and deletion of a tumor suppressor gene using the Cre/LoxP system (Figure S1A). Control cDNA (*GFP*) or murine *Sox2* were cloned into bicistronic lentiviral vectors under control of the β-*Actin* promoter (referred to as *Lenti-GFP-Cre* or *Lenti-Sox2-Cre*, respectively). Sox2 expression was validated by immunoblot analysis and Cre expression was verified using a human embryonic kidney 293T (HEK293T) reporter system that was used to calculate viral titer (Figures S1B and S1C).

Mice harboring conditional *LoxP*-flanked tumor suppressor alleles (*Lkb1*$^{fl/fl}$, *p53*$^{fl/fl}$, or *p53*$^{fl/fl}$*Rb*$^{fl/fl}$) were infected with *Lenti-GFP-Cre* or *Lenti-Sox2-Cre*. *LKB1* is lost or mutated in 5%–19% of human SCCs, but loss of *Lkb1* alone in the mouse lung does not lead to tumor formation (Ji et al., 2007). *TP53* is one of the most common genetic alterations in SCC (mutated in ~81% of tumors), but loss of *p53* alone in the mouse lung leads to rare adenocarcinomas after long latencies (Cancer Genome Atlas Research Network, 2012; Jackson et al., 2005; Meuwissen et al., 2003). Both *TP53* and *RB1* alterations are common in human SCLC (in which *SOX2* is genomically amplified in ~27% of cases), and loss of *p53*/*Rb* in the mouse lung leads to SCLC after long latencies, as well as rare adenocarcinomas (Cancer Genome Atlas Research Network, 2012; Meuwissen et al., 2003; Rudin et al., 2012). We reasoned that these tumor suppressor genes may cooperate with *Sox2* expression to promote lung tumor development. Beginning at 3 months postinfection, mice were monitored for tumor formation every month by low-dose microcomputed tomography (microCT) imaging for 7.5–12 months or until tumors were detected. The *Sox2-Lkb1* combination had the greatest reduction in tumor-free survival compared to other genetic combinations tested (Figure S1D). Individual tumors were observed by microCT in all three conditional genetic backgrounds and analyzed by histopathology (Figures 1A and 1B; Table 1). It is striking that most of the tumors in the *Lenti-Sox2-Cre Lkb1*$^{fl/fl}$ combination (n = 7 of 9 tumors in 17 mice) were classified as squamous tumors, as determined by analysis of hematoxylin and eosin (H&E)-stained sections by two independent pathologists (Figure 1B; Table 1). *Sox2-Lkb1* squamous tumors exhibited characteristic SCC features, including keratin pearls and desmoplastic stroma (Brcic et al., 2012) (Figure 1B). *Lkb1*$^{fl/fl}$ mice receiving *Lenti-GFP-Cre* did not develop tumors (n = 0 of 14 mice) as expected (Table 1). *Sox2* expression in the context of *p53* loss or loss of *p53*/*Rb* did not lead to squamous lung tumors, but it did lead to a few adenocarcinomas at latencies of 5–12 months (Table 1). The *Sox2-Lkb1* combination exhibited significantly increased tumor

Figure 1. *Lenti-Sox2;Lkb1*$^{fl/fl}$ Tumors Express Biomarkers of Human SCC

(A) Left panels: two representative microCT images with tumor outlined in dashed blue lines and heart outlined in solid red lines in axial view. Middle panels: three-dimensional microCT reconstructions (3D recon) with lung tumors in blue. Right panels: gross morphology of dissected lungs with tumors indicated by blue arrows. Mouse IDs (JC156 and JC163) correspond to tumors in Table 1.

(B) *Lenti-Sox2;Lkb1*$^{fl/fl}$ tumors and human SCC stained with H&E. Top scale bars represent 100 μM; bottom scale bars represent, 50 μM.

(C) Representative *Kras*$^{G12D/+}$ mouse lung adenocarcinomas, *Lenti-Sox2;Lkb1*$^{fl/fl}$ tumors, or human lung SCCs stained with K5, K14, p63, or TTF1. Scale bar represents 50 μM.

(D) Average IHC score based on 0–5 scoring system where 5 indicates >90% positive; 4 indicates >75%; 3 indicates >50%; 2 indicates >25%; 1 indicates >10%; and 0 indicates negative. Human SCCs (n = 12), tumors from Table 1, and *Kras*$^{G12D/+}$ adenocarcinomas were compared for K5, p63, and TTF1 IHC. Number of tumors analyzed is indicated in the color key. Error bars represent mean ± SEM. Student’s unpaired t test, *p = 0.02 for *Sox2/Lkb1* versus *Kras*, and p = 0.04 for *Sox2/Lkb1* versus human SCC.

See also Figure S1.

Table 1. *Lenti-Sox2;Lkb1*$^{fl/fl}$ Mice Develop Squamous Lung Tumors

Genotype	Virus delivered	No. of mice with tumors/ total mice	p value for tumor incidence Sox2 versus GFP	Mouse ID with tumor	Pathological review based on H&E (subtype after biomarker staining)	Biomarker staining	No. of squamous tumors/total tumors (based on biomarker staining)	Lkb1 recombination by PCR	Latency
Lkb1$^{fl/fl}$	*GFP*	0/14 (0%)					0/0 (0%)		6–10 months
	Sox2	7/17 (41%)	p = 0.009				8/9 (89%)		6–10 months
				JC156	squamous	K5+, K14+, p63+, Sox2+, TTF1 low		Yes	6 months, 5 days
				JC156b	squamous	n/a		n/a	6 months, 5 days
				JC163	squamous	K5+, K14+, p63+, Sox2+, TTF1+		Yes	7 months, 15 days
				JC163b	squamous	K5+, K14+, p63+, Sox2+, TTF1+		n/a	7 months, 15 days
				JC191	squamous	K5+, p63+, Sox2+, TTF1−		Yes	7 months, 9 days
				JC205	well-differentiated adenocarcinoma (squamous)	K5+, p63+, Sox2+		Yes	7 months, 5 days
				JC215	well-differentiated adenocarcinoma	K5−, p63−, Sox2+		Yes	9 months, 8 days
				JC217b	squamous	K5−, p63+, Sox2+, TTF1−		n/a	9 months, 12 days
				JC229	squamous	K5+, p63+, Sox2+, TTF1−		n/a	9 months, 18 days
p53$^{fl/fl}$	*GFP*	0/10 (0%)					0/0 (0%)		5.5–7.5 months
	Sox2	1/8 (11.1%)	p = 0.44				0/1 (0%)		5.5–7.5 months
				JC147	well-differentiated adenocarcinoma	K5-, p63−, Sox2-, TTF1+			5 months, 19 days
Rb$^{fl/fl}$*p53*$^{fl/fl}$	*GFP*	2/28 (7%)					0/2(0%)		6–12 months
				JC118	well-differentiated adenocarcinoma	n/a			6 months, 6 days
				JC204	poorly differentiated NSCLC (Adeno)	K5−, p63−, Sox2−, TTF1+			8 months, 12 days
	Sox2	2/14 (14%)	p = 0.59				0/3 (0%)		6–12 months
				JC189	well-differentiated adenocarcinoma	K5−, p63−, Sox2−, TTF1+			10 months, 27 days
				JC216	poorly differentiated NSCLC (Adeno)	K5−, p63−, Sox2−, TTF1+			12 months
				JC216b	poorly differentiated NSCLC (Adeno)	n/a			12 months

Detailed histopathology, biomarker staining, *Lkb1* recombination results, and latency of tumors are identified in mice receiving *GFP* or *Sox2* lentiviruses in indicated conditional genetic backgrounds. n/a indicates insufficient tissue available for analysis. See also Figure S1.

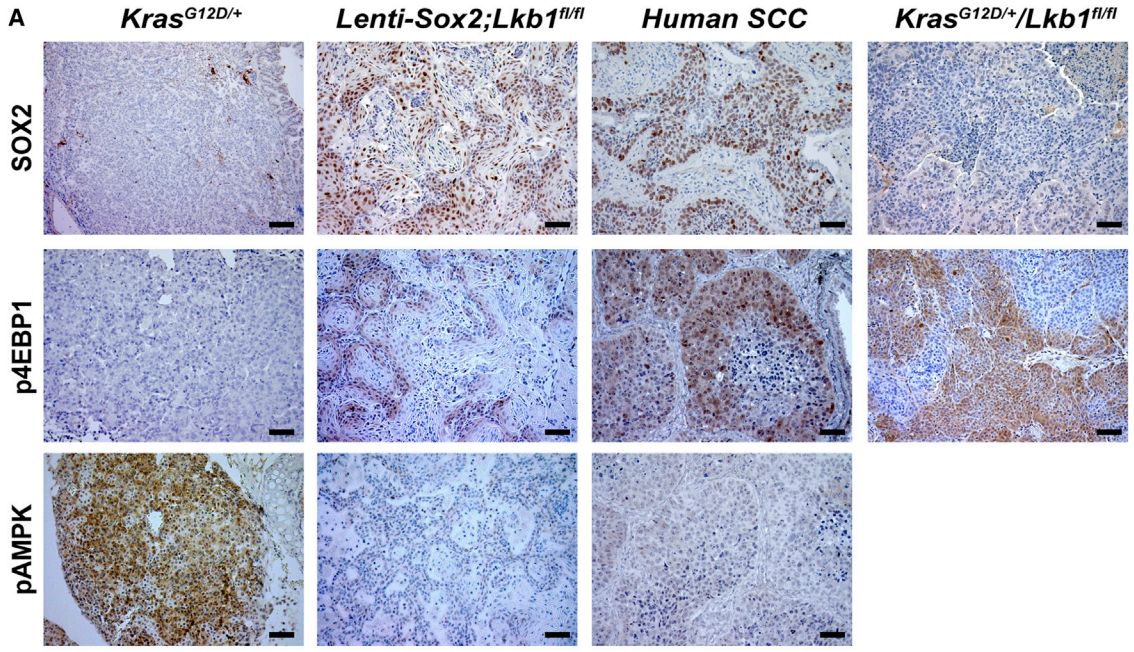

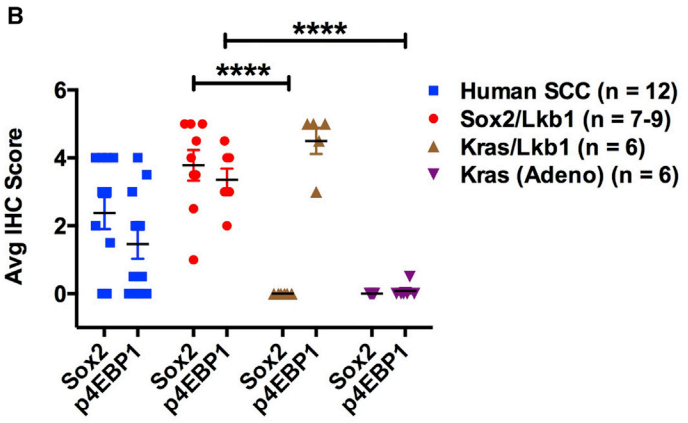

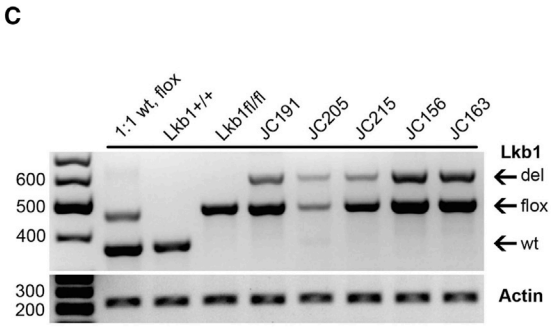

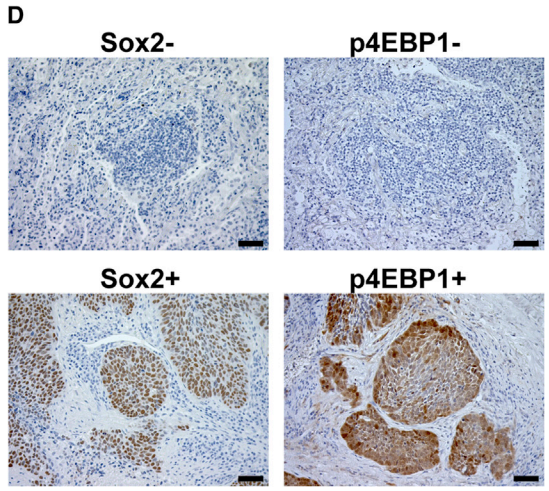

	p4EBP1-	p4EBP1+
Sox2-	2	1
Sox2+	4	5

(legend on next page)

incidence (Fisher's exact test, two sided, p = 0.009) and a significant enrichment in squamous tumors (89% versus 0%, Fisher's exact test, two sided, p = 0.001), compared to all other genetic combinations combined (Table 1). Together, these findings suggest that *Sox2* expression and *Lkb1* loss specifically cooperate to promote squamous tumorigenesis.

Lenti-Sox2-Cre Lkb1$^{fl/fl}$ Tumors Express Biomarkers of Human SCC

Expression of basal cell markers such as cytokeratin-5 (K5), -14 (K14), and P63 distinguish human SCC from adenocarcinoma (Reis-Filho et al., 2003; Terry et al., 2010). We analyzed tumors from each genetic combination, as well as 12 human SCCs for squamous biomarker expression. *Sox2-Lkb1* squamous tumors consistently expressed all of the basal cell markers examined (K5, K14, and p63) and were similar to human SCC, whereas adenocarcinomas in mice from other genetic combinations including *Kras^{G12D}* did not (Figures 1C and 1D; Figure S2; Table 1). Most human lung tumors express TTF1 (also known as Nkx2.1), but mean expression of TTF1 is significantly reduced in SCCs compared to adenocarcinomas and is reportedly expressed in only ~10% of SCCs (Perner et al., 2009). Compared to *Kras^{G12D}*-driven mouse adenocarcinomas that were uniformly TTF1 positive, TTF1 levels were significantly reduced in *Sox2-Lkb1* tumors (Student's unpaired t test, p = 0.02) (Figures 1C and 1D). *Sox2-Lkb1* tumors exhibited a broad spectrum of TTF1 expression, ranging from no TTF1 expression (similar to human SCCs) to higher levels of expression. *Sox2-Lkb1* tumors expressed significantly less TTF1 than mouse adenocarcinomas but significantly more TTF1 than human SCCs (Student's unpaired t test, p = 0.04) (Figures 1C and 1D). Taken together, these results demonstrate that *Sox2-Lkb1* tumors highly resemble human SCC at the level of histopathology and squamous biomarker expression.

Next, we sought to validate Sox2 expression and Lkb1 loss in mouse squamous tumors. All *Sox2-Lkb1* tumors were strongly positive for nuclear Sox2 expression, similar to 75% of human SCCs (n = 9 of 12) (Figures 2A and 2B). *Kras^{G12D}*-driven adenocarcinomas and adenocarcinomas arising from other genetic combinations (*p53* or *p53/Rb* loss) were negative for Sox2 (Figures 2A and 2B; Figure S2). Given that the same lentiviruses were used in all experiments, this suggests that there may be a selective advantage for high Sox2 expression in the context of *Lkb1* loss. It is interesting that *Kras$^{G12D/+}$Lkb1$^{fl/fl}$* squamous tumors had little or no Sox2 expression, suggesting that there may be Sox2-independent mechanisms of squamous tumorigenesis (Figures 2A and 2B). Recombination of the *Lkb1* allele was determined by PCR analysis on DNA from macrodissected *Sox2-Lkb1* tumors. All tumors examined (n = 5 of 5) demonstrated the presence of the recombined *Lkb1* floxed allele as well as Sox2 expression (Figure 2C; Table 1). Two of nine *Sox2-Lkb1* tumors appeared as adenocarcinomas by H&E, and both tumors exhibited Sox2 expression and *Lkb1* recombination; one tumor expressed basal cell markers and, as such, was reclassified by pathologists as squamous, whereas the other tumor did not express K5 or p63 (Table 1). This suggests that Sox2 expression and *Lkb1* loss may not be sufficient for squamous tumorigenesis in all contexts and/or that this adenocarcinoma represents an intermediate state that has the potential to transdifferentiate to a squamous tumor under certain conditions (Han et al., 2014).

LKB1 phosphorylates and activates adenosine monophosphate-activated protein kinase (AMPK), which negatively regulates the mammalian target of rapamycin (mTOR) pathway. Immunohistochemical (IHC) analysis of *Sox2-Lkb1* tumors demonstrated an absence of phosphorylated AMPK (pAMPK) and enhanced expression of phosphorylated eukaryotic translation initiation factor 4E-binding protein 1 (p4EBP1), an mTOR substrate (Hay and Sonenberg, 2004; Perner et al., 2009), confirming activation of the mTOR pathway (Figures 2A and 2B). The mTOR pathway is frequently activated in human lung SCCs and represents a potential therapeutic target (Mantripragada and Khurshid, 2013). Indeed, we observed that, of the human SCCs with strong SOX2 expression (9 of 12), five demonstrated evidence of mTOR pathway activation as well (55% of Sox2+ SCCs) (Figure 2D). Altogether, these data reveal that SOX2 expression and mTOR activity frequently co-occur in human SCC and that *Sox2-Lkb1* tumors strongly resemble human SCCs at the level of pathway activation.

Sox2-Driven SCCs Exhibit Expression or Activation of Potential Therapeutic Targets

To identify pathways dysregulated in *Sox2*-driven SCC, we performed IHC analysis for therapeutically relevant pathways in *Sox2-Lkb1* tumors, *Kras^{G12D}Lkb1$^{fl/fl}$* squamous tumors identified by K5 staining, and human SCCs. FGFR family members are frequently amplified and/or harbor activating point mutations in human SCC, and FGFR inhibitors are currently in clinical trials (Cancer Genome Atlas Research Network, 2012; Dutt et al., 2011; Liao et al., 2013). Notably, *SOX2* and *FGFR2* expression are highly correlated in human SCC, and SOX2 can bind the *FGFR2* promoter (Bass et al., 2009; Boyer et al., 2005; Fang et al., 2011), suggesting that *FGFR2* may be a direct target of SOX2 in lung cancer. We examined expression of FGFR2 in

Figure 2. *Lenti-Sox2;Lkb1$^{fl/fl}$* Tumors Express Sox2 and Exhibit Activation of the mTOR Pathway Similar to Human SCCs

(A) Representative IHC of Sox2, p4EBP1, and pAMPK in *Kras$^{G12D/+}$* mouse lung adenocarcinomas, *Lenti-Sox2;Lkb1$^{fl/fl}$* tumors, human lung SCCs, and *Kras$^{G12D/+}$Lkb1$^{fl/fl}$* squamous tumors. Brown/red staining is positive. Scale bar represents 50 μm.

(B) Average IHC scores for Sox2 and p4EBP1 from individual tumors indicated in Table 1 based on 0–5 scoring system where 5 indicates >90% positive; 4 indicates >75%; 3 indicates >50%; 2 indicates >25%; 1 indicates >10%; and 0 indicates negative. Number of tumors analyzed is indicated in color key at right. Error bars represent mean ± SEM. Student's unpaired t test, ****p < 0.001.

(C) PCR validation of *Lkb1* recombination in tumor samples from mice indicated in Table 1. Wild-type (WT), floxed (flox), and recombined (del) *Lkb1* alleles indicated. *Actin* serves as input control. Mixed 1:1 *Lkb1* WT and floxed DNA, *Lkb1$^{+/+}$*, and *Lkb1$^{fl/fl}$* normal lung DNA serve as controls.

(D) Left panels: representative images of Sox2- and p4EBP1-positive and -negative IHC. Right panels: contingency table of human SCCs (n = 12) stained with antibodies to SOX2 and p4EBP1.

See also Figure S2.

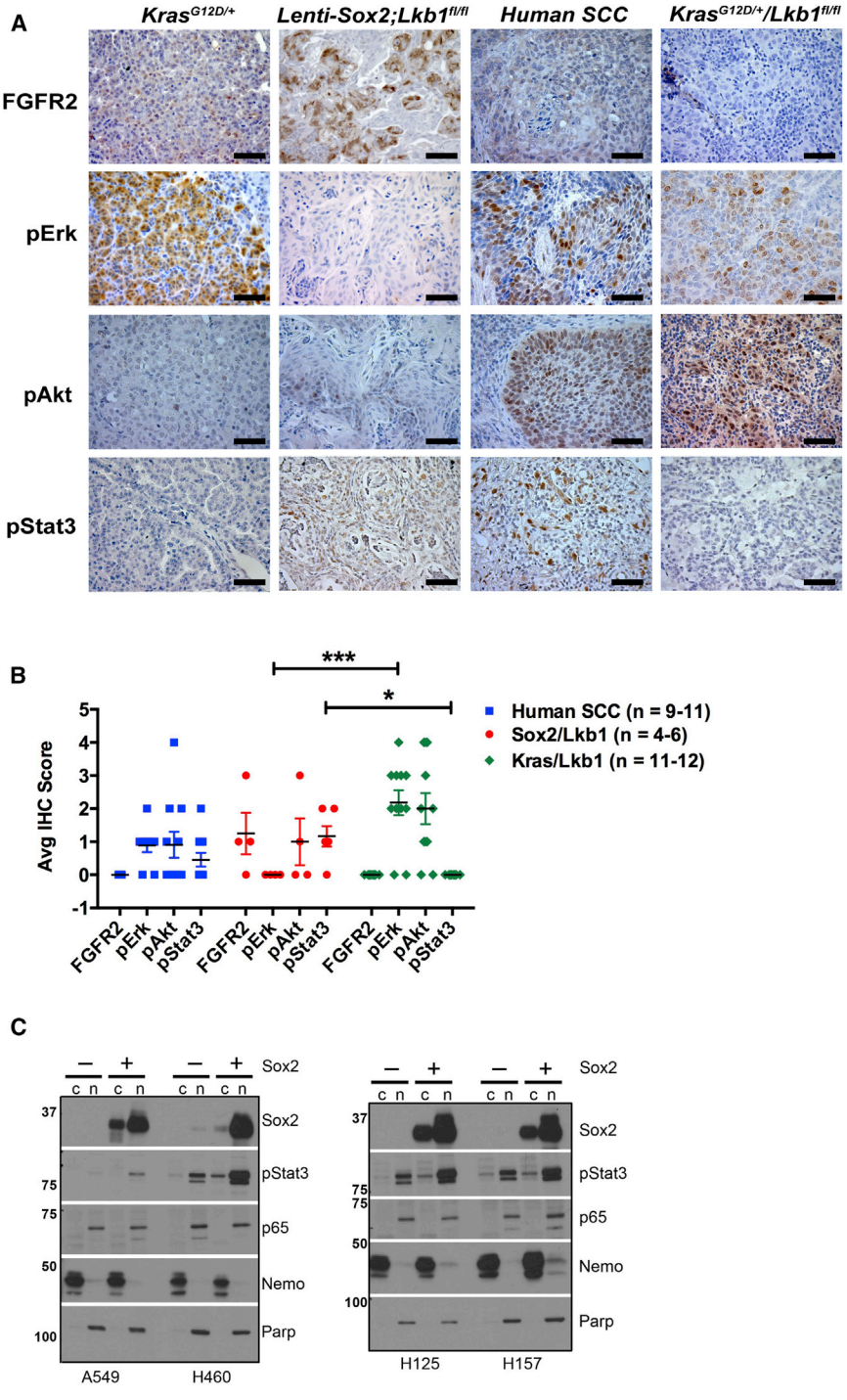

Figure 3. Murine SCCs Exhibit Expression of Potential Therapeutic Targets

(A) Representative IHC of *Kras*$^{G12D/+}$ mouse lung adenocarcinomas, mouse *Lenti-Sox2;Lkb1*$^{fl/fl}$ tumors, human lung SCCs, and *Kras*$^{G12D/+}$*Lkb1*$^{fl/fl}$ squamous tumors stained with indicated antibodies. Brown/red staining is positive. Scale bar represents 50 μm.

(B) Average IHC score of FGFR2, pErk, pAkt, and pStat3 stains in individual tumors from Table 1, human SCCs, and *Kras*$^{G12D/+}$*Lkb1*$^{fl/fl}$ squamous tumors. Number of tumors analyzed is indicated in color key at right. IHC scoring system is based on scoring system where 5 indicates >75% positive; 4 indicates >50%; 3 indicates >25%; 2 indicates >10%; 1 indicates >2.5%; and 0 indicates negative. Error bars represent mean ± SEM. For Student's unpaired t test, *** indicates $p < 0.0002$ and *$p < 0.01$.

(C) Immunoblot of cytoplasmic (c) and nuclear (n) protein extracts for SOX2, pStat3, and NF-κB p65 from human lung cancer cell lines under control (−) or 48 hr SOX2 induction (+) in stable Tet-On cells. Nemo and Parp serve as loading controls for cytoplasmic and nuclear fractions, respectively. See also Figure S3.

each tumor group and found that Fgfr2 expression tended to be higher in *Sox2-Lkb1* tumors compared to *Kras*^{G12D}*Lkb1*$^{fl/fl}$ squamous tumors, but these data did not reach statistical significance (Figures 3A and 3B). *FGFR2* was highly induced by SOX2 expression in human A549 lung cancer cells harboring *LKB1* mutations (Figure S3) but not in two other cell lines with *LKB1* mutations (H23 and H157) (Mahoney et al., 2009; Figure S3). We were not able to detect phospho-Frs or pFGFR2 in the *Sox2-Lkb1* tumors, so it remains to be determined whether pathways downstream of FGFR2 are activated.

The nuclear factor κB (NF-κB) pathway is activated and implicated in various cancers, including lung adenocarcinoma (Meylan et al., 2009; Xue et al., 2011) and lung SCC (Xiao et al., 2013). *Sox2-Lkb1* tumors demonstrated evidence of NF-κB pathway activity as indicated by nuclear p65, similar to *Kras*-driven adenocarcinomas (Figure S3). Although, the role of NF-κB signaling in SCC development remains to be determined, activation of this pathway in multiple mouse models of SCC warrants further study of NF-κB as a potential therapeutic target. Inducible SOX2 expression alone was not sufficient to increase nuclear p65 in human cell lines regardless of *LKB1* status, suggesting that other factors are likely driving NF-κB signaling in these cells (Figure 3C).

The RAS/MAPK/PI3K pathways are frequently activated in human squamous tumors via different mechanisms (Cancer Genome Atlas Research Network, 2012). To examine the status of these pathways, we stained tumors for pErk and pAkt. Notably, pErk was significantly reduced in *Sox2-Lkb1* tumors compared to *Kras*^{G12D}*Lkb1*$^{fl/fl}$ squamous tumors and human SCCs (Figures 3A and 3B). We speculate that Kras activation in *Kras*^{G12D}*Lkb1*$^{fl/fl}$ squamous tumors maintains pErk signaling,

which is absent in Sox2-driven tumors. We observed variable levels of pAkt in *Sox2-Lkb1* tumors, ranging from little or no pAkt to high levels similar to those in $Kras^{G12D}Lkb1^{fl/fl}$ tumors (Figures 3A and 3B). Together, *Sox2-Lkb1* tumors had reduced MAPK pathway activity compared to $Kras^{G12D}Lkb1^{fl/fl}$ squamous tumors, suggesting that *Sox2-Lkb1* tumors may rely more heavily on other growth factor signaling pathways for proliferation, including mTOR. A recent study published while this article was under consideration demonstrated that *Pten* loss cooperates with *Lkb1* loss to promote SCC (Xu et al., 2014). Notably, *Pten/Lkb1*-null tumors also exhibited low MAPK pathway activation.

Stat3 has been shown to cooperate with Sox2 to promote tumor progression in esophageal and forestomach tumors, cancers in which *SOX2* is genomically amplified (Liu et al., 2013). Preclinical studies have identified STAT3 inhibitors, and STAT3 decoys are now being tested in patients with head and neck SCC (Sen et al., 2012). Compared to $Kras^{G12D}$ adenocarcinomas and $Kras^{G12D}Lkb1^{fl/fl}$ squamous tumors, the Jak-Stat pathway was significantly activated in *Sox2-Lkb1* tumors (indicated by phospho-Stat3) with clear nuclear pStat3 in some cells within the squamous tumors (Figures 3A and 3B). Human SCCs had variable levels of pStat3 similar to those in *Sox2-Lkb1* tumors (Figures 3A and 3B). It is striking that, in multiple human lung cancer cell lines of adenocarcinoma and squamous lineage, inducible expression of SOX2 consistently promoted nuclear pStat3 accumulation (Figure 3C). Altogether, these data suggest that Sox2 contributes to Stat signaling in vivo and thus represents a therapeutic target warranting further investigation for SCC treatment.

To summarize, we have used a lentiviral-based approach to generate a mouse model of SCC based on *Sox2* expression and *Lkb1* loss, highlighting their cooperation in lung SCC development. Both SOX2 expression and mTOR pathway activity frequently co-occur in human SCC, making this model particularly relevant to the human disease. Mouse tumors recapitulate the human disease at the level of histopathology, biomarker expression, and activation of potential therapeutic targets that have been largely unexplored in SCC treatment. It is important to note that Stat signaling was induced by SOX2 in vitro and enriched in Sox2-driven squamous tumors. This model thus serves as a preclinical tool to test whether STAT inhibition is therapeutically effective against Sox2-driven SCCs.

The low penetrance of tumor formation in this model may be due to low lentiviral titer and/or the underlying cell of origin. Although we recognize that tumor numbers in this study are low, the paucity of other squamous lung tumor models suggests that this particular genetic combination is highly relevant. While this article was under consideration, Xu et al. demonstrated that *Pten/Lkb1* loss promotes squamous lung tumors exclusively, in contrast to *Kras/Lkb1* mice, which develop multiple tumor types (Ji et al., 2007; Xu et al., 2014). It remains unknown why PI3K activation, as opposed to MAPK, would lead exclusively to squamous tumors in the context of *Lkb1* loss, especially since PI3K pathway alterations also occur in adenocarcinoma (Ding et al., 2008). We speculate that, since *Pten/Lkb1*-null tumors express Sox2, Sox2 may be a critical target of the PI3K pathway in these tumors.

In both *Pten/Lkb1* and *Sox2/Lkb1* mouse models, inflammatory microenvironment and activation of immune signaling pathways appear to distinguish SCC from adenocarcinoma (Xu et al., 2014). A notable difference between the two models is that adenoviruses used in *Pten/Lkb1* and *Kras/Lkb1* models are thought to enhance inflammation compared to lentiviruses used here. These models will serve as preclinical tools for further investigation of immunotherapy efficacy and function.

It is unclear whether SCCs arise from basal cells or whether the transforming events promote basal cell differentiation. The identity of the cell of origin for SCC remains an important unanswered question. One model suggests that basal cells serve as the cells of origin because SCCs express basal cell markers and Sox2 is expressed in basal cells (Que et al., 2009; Sutherland and Berns, 2010). However, other studies suggest that Sox2 promotes basal cell fate (Han et al., 2014; Lu et al., 2010). Recent studies in $Kras^{G12D/+}Lkb1^{fl/fl}$ mice suggest that type II pneumocyte-derived lung adenocarcinomas can transdifferentiate into SCCs (Han et al., 2014). Given that lentiviruses in our model may target multiple cell types in the mouse lung, it is possible that Sox2 expression and *Lkb1* loss are capable of altering cell fate to a squamous-like identity. Given that we also detected one tumor that appeared as an adenocarcinoma expressing basal cell markers, we speculate that transdifferentiation may also occur in this model. The lentiviral approach used here could be adapted to investigate the cell of origin for Sox2-driven SCCs.

Bicistronic lentiviruses may also be used to test other candidate SCC drivers, such as *P63* and *NRF2*, as well as to identify cooperating genetic events that promote SCC. We expect that murine squamous tumors will have fewer "passenger" genetic alterations than human SCC due to lack of carcinogen exposure, thereby providing a biological filter to identify "driver" genetic changes in SCC. Beyond lung cancer, findings from this model may have important clinical implications for other squamous or SOX2-driven malignancies such as SCLC and brain, esophageal, and oral cancers.

EXPERIMENTAL PROCEDURES

Mouse Breeding and Lentiviral Infections

Mice were housed in an environmentally controlled room according to the Committee of Animal Care. $Lkb1^{fl/fl}$ mice were purchased from The Jackson Laboratory. $LSL\text{-}Kras^{G12D/+}$ and $p53^{fl/fl}$ animals were kindly provided by Tyler Jacks. $p53^{fl/fl}Rb^{fl/fl}$ mice were generated by Anton Berns (Meuwissen et al., 2003) and obtained from T. Jacks. Lung tumor tissue from $Kras^{G12D/+}Lkb1^{fl/fl}$ mice was kindly provided by Reuben Shaw. At 6–8 weeks of age, anesthetized mice were infected with $\sim 10^7$ infectious units/ml of *Lenti-Sox2-Cre* or *GFP-Cre* lentiviruses or 6.47×10^7 plaque-forming units of AdCre (University of Iowa) by nasal instillation as described elsewhere (Jackson et al., 2001). Viruses were administered in a Biosafety Level 2+ room according to Institutional Biosafety Committee guidelines.

Lentivirus Production

GFP and murine *Sox2* cDNAs were cloned into bicistronic lentiviral vectors expressing *Cre* to generate *Lenti-Sox2-Cre* and *Lenti-GFP-Cre* plasmids and confirmed by direct sequencing. 293T cells were transfected with a three-plasmid transfection system including the lentiviral vector, pCMV-delta-8.2 (Addgene) and pCMV-VSV-G (Addgene). Virus was harvested posttransfection, concentrated by ultracentrifugation (24,000 × *g*), and titered using HEK293T reporter cells stably expressing a *Lox-DsRed2(Stop)-Lox-GFP*

cassette. Number of cells expressing green fluorescent protein was measured by flow cytometry and used to calculate titer (infectious U/ml).

MicroCT Imaging

At indicated time points, mice were scanned for 30 s to 2 min under isoflurane anesthesia using a small animal Quantum FX microCT (PerkinElmer) at 45 υm resolution, 90 kV, with 160 υA current. Images were acquired using PerkinElmer Quantum FX software and processed with Analyze 11.0 (AnalyzeDirect).

Human Tissue

Excess deidentified fresh tissue was obtained with prior patient consent under approved protocol by the institutional review board (#10924). Institutional guidelines regarding specimen use were followed.

SUPPLEMENTAL INFORMATION

Supplemental Information includes Supplemental Experimental Procedures and three figures and can be found with this article online at http://dx.doi.org/10.1016/j.celrep.2014.05.036.

AUTHOR CONTRIBUTIONS

A.M. designed and performed the majority of experiments, acquired and analyzed data, and wrote the manuscript. K.B., U.K., P.C., and S.P. performed experiments. S.C provided human tissue. B.W. and S.C. analyzed histopathology and provided clinical expertise. T.O. conceived of the project, analyzed the data, and wrote the paper.

ACKNOWLEDGMENTS

We thank Drs. W. Akerley, S. Slomowitz, and A.J. Bhutkar for valuable advice and Dr. K. Jones for critical reading of the manuscript. We are especially grateful to Dr. R. Shaw for providing *Kras/Lkb1* tissue. Thanks to members of the T.G.O. Lab for technical support, especially M. Terry, R. Arya, and J. Clegg. We thank Y. Derose, B. Anderson, and K. Gligorich for histological services; M. DuPage, K. Lane, and the T. Jacks laboratory for lentiviral constructs; and M. Van Brocklin for HEK293T reporter cells. T.G.O. was supported in part by a Department of Defense Lung Concept Award (DoD USAMRAA W81XWH-12-1-0211) and a V Scholar award from The V Foundation for Cancer Research. T.G.O. is a Damon Runyon-Rachleff Innovation Awardee supported in part by the Damon Runyon Cancer Research Foundation (DRR-26-13).

Received: March 14, 2014
Revised: April 26, 2014
Accepted: May 18, 2014
Published: June 19, 2014

REFERENCES

Bass, A.J., Watanabe, H., Mermel, C.H., Yu, S., Perner, S., Verhaak, R.G., Kim, S.Y., Wardwell, L., Tamayo, P., Gat-Viks, I., et al. (2009). SOX2 is an amplified lineage-survival oncogene in lung and esophageal squamous cell carcinomas. Nat. Genet. *41*, 1238–1242.

Boyer, L.A., Lee, T.I., Cole, M.F., Johnstone, S.E., Levine, S.S., Zucker, J.P., Guenther, M.G., Kumar, R.M., Murray, H.L., Jenner, R.G., et al. (2005). Core transcriptional regulatory circuitry in human embryonic stem cells. Cell *122*, 947–956.

Brcic, L., Sherer, C.K., Shuai, Y., Hornick, J.L., Chirieac, L.R., and Dacic, S. (2012). Morphologic and clinicopathologic features of lung squamous cell carcinomas expressing Sox2. Am. J. Clin. Pathol. *138*, 712–718.

Cancer Genome Atlas Research Network (2012). Comprehensive genomic characterization of squamous cell lung cancers. Nature *489*, 519–525.

Ding, L., Getz, G., Wheeler, D.A., Mardis, E.R., McLellan, M.D., Cibulskis, K., Sougnez, C., Greulich, H., Muzny, D.M., Morgan, M.B., et al. (2008). Somatic mutations affect key pathways in lung adenocarcinoma. Nature *455*, 1069–1075.

Dutt, A., Ramos, A.H., Hammerman, P.S., Mermel, C., Cho, J., Sharifnia, T., Chande, A., Tanaka, K.E., Stransky, N., Greulich, H., et al. (2011). Inhibitor-sensitive FGFR1 amplification in human non-small cell lung cancer. PLoS ONE *6*, e20351.

Fang, X., Yoon, J.G., Li, L., Yu, W., Shao, J., Hua, D., Zheng, S., Hood, L., Goodlett, D.R., Foltz, G., and Lin, B. (2011). The SOX2 response program in glioblastoma multiforme: an integrated ChIP-seq, expression microarray, and microRNA analysis. BMC Genomics *12*, 11.

Gontan, C., de Munck, A., Vermeij, M., Grosveld, F., Tibboel, D., and Rottier, R. (2008). Sox2 is important for two crucial processes in lung development: branching morphogenesis and epithelial cell differentiation. Dev. Biol. *317*, 296–309.

Han, X., Li, F., Fang, Z., Gao, Y., Li, F., Fang, R., Yao, S., Sun, Y., Li, L., Zhang, W., et al. (2014). Transdifferentiation of lung adenocarcinoma in mice with Lkb1 deficiency to squamous cell carcinoma. Nat Commun *5*, 3261.

Hay, N., and Sonenberg, N. (2004). Upstream and downstream of mTOR. Genes Dev. *18*, 1926–1945.

Hussenet, T., Dali, S., Exinger, J., Monga, B., Jost, B., Dembelé, D., Martinet, N., Thibault, C., Huelsken, J., Brambilla, E., and du Manoir, S. (2010). SOX2 is an oncogene activated by recurrent 3q26.3 amplifications in human lung squamous cell carcinomas. PLoS ONE *5*, e8960.

Jackson, E.L., Willis, N., Mercer, K., Bronson, R.T., Crowley, D., Montoya, R., Jacks, T., and Tuveson, D.A. (2001). Analysis of lung tumor initiation and progression using conditional expression of oncogenic K-ras. Genes Dev. *15*, 3243–3248.

Jackson, E.L., Olive, K.P., Tuveson, D.A., Bronson, R., Crowley, D., Brown, M., and Jacks, T. (2005). The differential effects of mutant p53 alleles on advanced murine lung cancer. Cancer Res. *65*, 10280–10288.

Jemal, A., Bray, F., Center, M.M., Ferlay, J., Ward, E., and Forman, D. (2011). Global cancer statistics. CA Cancer J. Clin. *61*, 69–90.

Ji, H., Ramsey, M.R., Hayes, D.N., Fan, C., McNamara, K., Kozlowski, P., Torrice, C., Wu, M.C., Shimamura, T., Perera, S.A., et al. (2007). LKB1 modulates lung cancer differentiation and metastasis. Nature *448*, 807–810.

Kwon, M.C., and Berns, A. (2013). Mouse models for lung cancer. Mol. Oncol. *7*, 165–177.

Liao, R.G., Jung, J., Tchaicha, J., Wilkerson, M.D., Sivachenko, A., Beauchamp, E.M., Liu, Q., Pugh, T.J., Pedamallu, C.S., Hayes, D.N., et al. (2013). Inhibitor-sensitive FGFR2 and FGFR3 mutations in lung squamous cell carcinoma. Cancer Res. *73*, 5195–5205.

Liu, S., Chen, Z., Zhu, F., and Hu, Y. (2012). IκB kinase alpha and cancer. J. Interferon Cytokine Res. *32*, 152–158.

Liu, K., Jiang, M., Lu, Y., Chen, H., Sun, J., Wu, S., Ku, W.Y., Nakagawa, H., Kita, Y., Natsugoe, S., et al. (2013). Sox2 cooperates with inflammation-mediated Stat3 activation in the malignant transformation of foregut basal progenitor cells. Cell Stem Cell *12*, 304–315.

Lu, Y., Futtner, C., Rock, J.R., Xu, X., Whitworth, W., Hogan, B.L., and Onaitis, M.W. (2010). Evidence that SOX2 overexpression is oncogenic in the lung. PLoS ONE *5*, e11022.

Mahoney, C.L., Choudhury, B., Davies, H., Edkins, S., Greenman, C., Haaften, Gv., Mironenko, T., Santarius, T., Stevens, C., Stratton, M.R., and Futreal, P.A. (2009). LKB1/KRAS mutant lung cancers constitute a genetic subset of NSCLC with increased sensitivity to MAPK and mTOR signalling inhibition. Br. J. Cancer *100*, 370–375.

Mantripragada, K., and Khurshid, H. (2013). Targeting genomic alterations in squamous cell lung cancer. Front Oncol *3*, 195.

Meuwissen, R., Linn, S.C., Linnoila, R.I., Zevenhoven, J., Mooi, W.J., and Berns, A. (2003). Induction of small cell lung cancer by somatic inactivation of both Trp53 and Rb1 in a conditional mouse model. Cancer Cell *4*, 181–189.

Meylan, E., Dooley, A.L., Feldser, D.M., Shen, L., Turk, E., Ouyang, C., and Jacks, T. (2009). Requirement for NF-kappaB signalling in a mouse model of lung adenocarcinoma. Nature *462*, 104–107.

Oliver, T.G., Patel, J., and Akerley, W. (2013). Squamous non-small cell lung cancer as a distinct clinical entity. Am. J. Clin. Oncol., Published online July 24, 2013 http://dx.doi.org/10.1097/COC.0b013e3182a0e850.

Perez-Moreno, P., Brambilla, E., Thomas, R., and Soria, J.C. (2012). Squamous cell carcinoma of the lung: molecular subtypes and therapeutic opportunities. Clin. Cancer Res. *18*, 2443–2451.

Perner, S., Wagner, P.L., Soltermann, A., LaFargue, C., Tischler, V., Weir, B.A., Weder, W., Meyerson, M., Giordano, T.J., Moch, H., and Rubin, M.A. (2009). TTF1 expression in non-small cell lung carcinoma: association with TTF1 gene amplification and improved survival. J. Pathol. *217*, 65–72.

Que, J., Luo, X., Schwartz, R.J., and Hogan, B.L. (2009). Multiple roles for Sox2 in the developing and adult mouse trachea. Development *136*, 1899–1907.

Reis-Filho, J.S., Simpson, P.T., Martins, A., Preto, A., Gärtner, F., and Schmitt, F.C. (2003). Distribution of p63, cytokeratins 5/6 and cytokeratin 14 in 51 normal and 400 neoplastic human tissue samples using TARP-4 multi-tumor tissue microarray. Virchows Arch. *443*, 122–132.

Rudin, C.M., Durinck, S., Stawiski, E.W., Poirier, J.T., Modrusan, Z., Shames, D.S., Bergbower, E.A., Guan, Y., Shin, J., Guillory, J., et al. (2012). Comprehensive genomic analysis identifies SOX2 as a frequently amplified gene in small-cell lung cancer. Nat. Genet. *44*, 1111–1116.

Sen, M., Thomas, S.M., Kim, S., Yeh, J.I., Ferris, R.L., Johnson, J.T., Duvvuri, U., Lee, J., Sahu, N., Joyce, S., et al. (2012). First-in-human trial of a STAT3 decoy oligonucleotide in head and neck tumors: implications for cancer therapy. Cancer Discov *2*, 694–705.

Shackelford, D.B., and Shaw, R.J. (2009). The LKB1-AMPK pathway: metabolism and growth control in tumour suppression. Nat. Rev. Cancer *9*, 563–575.

Sutherland, K.D., and Berns, A. (2010). Cell of origin of lung cancer. Mol. Oncol. *4*, 397–403.

Terry, J., Leung, S., Laskin, J., Leslie, K.O., Gown, A.M., and Ionescu, D.N. (2010). Optimal immunohistochemical markers for distinguishing lung adenocarcinomas from squamous cell carcinomas in small tumor samples. Am. J. Surg. Pathol. *34*, 1805–1811.

Xiao, Z., Jiang, Q., Willette-Brown, J., Xi, S., Zhu, F., Burkett, S., Back, T., Song, N.Y., Datla, M., Sun, Z., et al. (2013). The pivotal role of IKKα in the development of spontaneous lung squamous cell carcinomas. Cancer Cell *23*, 527–540.

Xu, C., Fillmore, C.M., Koyama, S., Wu, H., Zhao, Y., Chen, Z., Herter-Sprie, G.S., Akbay, E.A., Tchaicha, J.H., Altabef, A., et al. (2014). Loss of Lkb1 and Pten leads to lung squamous cell carcinoma with elevated PD-L1 expression. Cancer Cell *25*, 590–604.

Xue, W., Meylan, E., Oliver, T.G., Feldser, D.M., Winslow, M.M., Bronson, R., and Jacks, T. (2011). Response and resistance to NF-κB inhibitors in mouse models of lung adenocarcinoma. Cancer Discov *1*, 236–247.